ARTICLE TITLE

A Synthetic Tunable Amplifying Buffer Circuit in *E. coli*

AUTHORS

Kayzad Soli Nilgiriwala[1], José Jiménez[1,2], Phillip Michael Rivera[1], and Domitilla Del Vecchio[1,*]

ADDRESSES

[1]Department of Mechanical Engineering,

Massachusetts Institute of Technology,

77 Massachusetts Avenue,

Cambridge, MA02139-4307, USA.

[2]Present address: Faculty of Health and Medical Sciences, University of Surrey,

Guildford, Surrey GU2 7XH, UK.

*CORRESPONDING AUTHOR

Prof. Domitilla Del Vecchio

Room 3-455B, Department of Mechanical Engineering,

Massachusetts Institute of Technology,

77 Massachusetts Avenue, Cambridge, MA 02139-4307, USA.

Phone: +1-617-452-2275.

E-mail: ddv@mit.edu

Abstract

While predictable design of a genetic circuit's output is a major goal of synthetic biology, it remains a significant challenge because DNA binding sites in the cell affect the concentration of available transcription factors (TF). To mitigate this problem, we propose to use a TF that results from the (reversible) phosphorylation of protein substrate as a circuit's output. We demonstrate that by comparatively increasing the amounts of substrate and phosphatase, the TF concentration becomes robust to the presence of DNA binding sites and can be kept at a desired value. The circuit's input/output gain can in turn be tuned by changing the relative amounts of the substrate and phosphatase, realizing an amplifying buffer circuit with tunable gain. In our experiments in *E. coli,* we employ phospho-NRI as the output TF, phosphorylated by the NRII kinase and dephosphorylated by the NRII phosphatase. Amplifying buffer circuits such as ours could be used to insulate a circuit's output from the context, bringing synthetic biology one step closer to modular design.

Keywords

INTRODUCTION

A major goal of synthetic biology is to create a library of devices whose output is essentially independent of the device's connectivity and context.[1-3] The output of a device is usually a TF, which binds both, specifically to sites on the promoters that it regulates and non-specifically to a large number of additional DNA sites in the cell.[4] It has been demonstrated theoretically and experimentally that the concentration of a TF is substantially affected by the DNA sites to which it binds.[5-9] Experiments in *E. coli* have shown that DNA binding sites can cause a substantial slowdown of the temporal response of a device's output to input stimuli.[6] The steady state response of a device's output is especially affected by DNA binding sites, with resulting phenomena such as ultrasensitivity and thresholding.[7-9] In general, the dependence of a gene's input/output relation on the targets of the output has been termed ''retroactivity'' to generalize the concept of loading to non-electrical circuits.[5, 10] Because of retroactivity, the output of a genetic device may vary significantly depending on the context, which includes the connectivity to other devices and the specific bacterial strain.[11] This fact requires to re-optimize a circuit whenever it is placed in a different context, leading to a lengthy design process.

Here, we demonstrate that the steady state concentration of a TF can be rendered practically insensitive to the presence of DNA binding sites if such a TF results from the kinase-mediated reversible phosphorylation of an otherwise inactive protein substrate (Fig. 1A). Increased values of substrate lead to larger output values for the same kinase concentration and, as a consequence, the DNA binding sites have less of an effect on the concentration of the output TF. However, larger amounts of substrate lead to increased values of the input/output "gain" of the dose response curve from kinase concentration to TF concentration. The original gain can be restored by increasing the concentration of phosphatase. In summary, by comparatively increasing the amounts of substrate and phosphatase, we make a prescribed input/output dose response curve robust to the presence of the output TF DNA binding sites (Fig. 1B).

Hundreds of two-component signaling systems (TCSs) have been discovered in bacteria and many of them have been studied in great depth over the past few decades.[12-18] These TCSs form an essential component of signaling systems and play an indispensable role in the survival and proliferation of all prokaryotes beyond any doubt. In a TCS, signal is received and transmitted by the sensor kinase (SK) protein, which is usually a membrane bound homodimeric protein kinase that autophosphorylates itself.[19] Following the input signal and autophosphorylation of the kinase, the phosphoryl group is transferred to the response regulator (RR), which in turn activates the expression of the required genes. The amplifying buffer circuit that we propose in this paper is based on one of the essential and most studied TCS that forms the backbone of nitrogen regulation in *Escherichia coli* and which is responsible for regulating around 2% of the chromosomal genes during a nitrogen stress response,[20] indicating that it may naturally encounter substantial retroactivity. We chose this system as its behavior has been studied extensively and

the underlying molecular mechanisms and biochemical parameters have been well characterized.[19, 21-23] We constructed a synthetic NtrB-NtrC (SK-RR) phosphorylation cycle wherein the RR NRI can be expressed at four different levels and the NRII phosphatase can be induced via IPTG. We then examined the dose response curve by inducing the NRII kinase via aTc and measuring the concentration of phospho-NRI through a GFP reporter, in the presence and absence of phospho-NRI DNA binding sites, for high and low values of NRI and NRII phosphatase concentrations.

RESULTS AND DISCUSSION

1. Toy Model

To illustrate the main design principle that confers robustness of the output TF to the presence of DNA binding sites (Fig. 1A), it is sufficient to consider a one-step reaction model for the two enzymatic reactions of the phosphorylation cycle (see Supplementary Information, section 2.1). Referring to Fig. 1A and letting italics denote species concentration, we can write the rate of change of the output X^* as:

$$\frac{dX^*}{dt} = k_1 Z(X_{tot} - X^* - C) - k_2 Y_{tot} X^* - k_{on} X^*(p_{tot} - C) + k_{off} C$$

$$\frac{dC}{dt} = k_{on} X^*(p_{tot} - C) - k_{off} C$$

in which p_{tot} is the total concentration of DNA promoter sites (the load), to which X^* binds with association and dissociation rate constants given by k_{on} and k_{off}, respectively, to form the complex C. Here, k_1 and k_2 are the rate constants of the enzymatic reactions, while X_{tot} and Y_{tot} are the total amounts of substrate and phosphatase, respectively. The concentration Z of the kinase is bounded above by a value that depends on the strength of the inducible promoter that controls the expression of Z. In particular, we will have $Z = F(U)$, in which F is the standard Hill function. The steady state value of X^* can be obtained by setting the time derivatives to zero and by letting, for simplifying exposition, the DNA binding sites be saturated by the TF X^*, so that $C \simeq p_{tot}$ (see Supplementary Information, section 2.1 for the general case). In this case, we have that

$$X^* = \frac{k_1 X_{tot} Z}{k_2 Y_{tot} + k_1 Z} - \frac{k_1 p_{tot} Z}{k_2 Y_{tot} + k_1 Z}$$

which, for X_{tot} and Y_{tot} sufficiently large is well approximated by the form illustrated in Fig. 1B with $load = k_1 p_{tot} Z$. Specifically, we see from this expression that as X_{tot} increases, the first term becomes larger compared to the second term, so that the effect of the load on the output X^* becomes smaller. However, by increasing X_{tot}, the gain $\frac{k_1 X_{tot}}{k_2 Y_{tot}}$ from Z to X^* also increases. To keep this gain at a desired value, we can also increase the amount of phosphatase Y_{tot}, such that we ultimately obtain

$$X^* \simeq \frac{k_1 X_{tot}}{k_2 Y_{tot}} F(U) \tag{1}$$

which is independent of the load.

Since the key parameters that control the attenuation of the load and the system's gain are X_{tot} and Y_{tot}, we realized the system in Fig. 1A through a genetic circuit

where the amounts of the substrate X and phosphatase Y can be tuned. This is explained in the next section.

2. The circuit

We constructed four individual gene circuits. Each circuit is composed of a constitutively expressed *ntrC* gene leading to production of a constant amount of NRI protein substrate. The kinase [*ntrB*, NRII(L16R)][24] and phosphatase [*ntrB*, NRII(H139N)][25] genes are regulated by the repressors TetR and LacI, respectively, and induced by anhydrotetracycline (aTc) and isopropyl β-D-1-thiogalactopyranoside (IPTG), respectively. Phospho-NRI (NRI*) is detected using a reporter gene (superfolder green fluorescent protein; sf-*gfp*), which has an upstream P*glnA2* enhancer-promoter DNA sequence (Fig. 2). All the circuit genes are cloned in a medium copy number plasmid pACYC184 (20-30 copies per cell) at various restriction enzyme sites (Supplementary information sections 1.1-1.3; Supplementary Figs. S1 – S4). The DNA load (to the system output) used in this study is composed of two identical, strong binding sites (enhancer site-2) of the P*glnA2* promoter/enhancer cloned in pUC19 plasmid. Four such circuit plasmids were constructed, wherein the NRI was constitutively expressed at four different relative concentrations: very low (VL), low (L), medium (M), and high (H). These different concentrations were obtained by the following different combinations of the promoter and the ribosome binding site (RBS): P(21)RBS(34) for VL NRI (very low NRI), P(256)RBS(32) for L NRI (medium NRI), P(162)RBS(34) for M NRI (medium NRI) and P(256)RBS(34) for H NRI (high NRI). The details of the relative strengths of the RBSs used for the various circuit parts (Table S5) and their construction are provided in the materials and methods.

Each circuit plasmid was co-transformed with either the DNA load plasmid to test the effect of DNA load in the system or with an empty pUC19 plasmid as a control circuit without any DNA load inserted. As a result, we obtained eight different systems with increasing amounts of NRI, each with the DNA load or without it, leading to increasing values of the input amplification. In the systems with low, medium, and high NRI, the NRII phosphatase can be induced by the addition of IPTG, providing a mechanism to increase the strength of the negative feedback (Fig. 2).

3. Input/output dose response curve

The four individual circuits producing different amounts of NRI, without and with DNA load, were induced with aTc to obtain increasing amounts of NRII kinase, which leads to phosphorylation of the NRI substrate. The circuit was induced with different aTc concentrations and for each of these, cells were allowed to reach a steady state fluorescence to obtain the dose response curve of GFP to aTc (indicating NRI* concentration). The dose response curves for low (L) and medium (M) amounts of the NRI substrate, with and without DNA load, are shown in Fig. 3A,B (see Supplementary Information, section 1.4 and Supplementary Fig. S5). Since the circuits with very low and low NRI both showed the effect of retroactivity, and

the circuits with medium and high NRI showed attenuation of retroactivity, the circuits with low and medium NRI were considered as representatives for retroactive behavior and its attenuation. The fluorescence was measured by flow cytometry in all the cases (see Supplementary Figs. S6-S9). For the low NRI amount, the DNA load exerted a dramatic effect by reducing the GFP steady state levels at all aTc, and hence kinase, levels (Fig. 3A). An increase in NRI increased the steady state fluorescence and in turn reduced the effect of the DNA load as expected (Fig. 3B). Hence, by increasing the substrate (NRI) amount, we achieved robustness of the NRI* concentration (system output) to DNA load but this increased the NRII kinase-to-NRI* gain (according to equation (1)), resulting in the observed dose response curve with higher values of fluorescence for all aTc values. To recover the original input/output steady state characteristic shown in Fig. 3A (black), we induced the NRII phosphatase with 80 μM IPTG. As expected from the model, the input/output steady state characteristic approached the original one, while the system preserved its ability to attenuate the effect of the DNA load (Fig. 3C). Figure 3D and the insets in Fig. 3AB show simulation results performed on an ODE model that includes all the known molecular interactions present in the system with parameter values obtained from the literature (Supplementary Information, sections 3.1 – 3.3). The simulation results correlated well with the data.

This result indicates that the ability of this system of attenuating the effect of the DNA load on the output is due to the synergy between the negative feedback and the input amplification as explained in Section 1. This design hence enables to achieve robustness of the output TF to DNA load while leaving the freedom of attaining a desired input/output steady state response. While without negative feedback (no IPTG induction of the NRI phosphatase), the only way to decrease the influence of the DNA load on the output is to trivially increase the output itself (Fig. 3AB), the presence of negative feedback does not require to increase the output level to attain robustness to loading by DNA (Fig. 3C). It hence allows to decouple the specification on the input/output gain from that of robustness to DNA load.

4. Tradeoffs with dynamic response

The molecular mechanism that allows the NRII kinase to phosphorylate the NRI substrate (Fig. 2) involves binding of the kinase onto the substrate. Just like DNA binding sites apply a load to the output transcription factor NRI*, the binding sites on the NRI substrate apply a load to the NRII kinase. It is known that this substrate load decreases the free availability of kinase and slows down the kinases' temporal dynamics[5] (Supplementary Information, section 3.5.2). These facts have been experimentally verified on a covalent modification cycle reconstituted *in vitro*.[26] Since increased amounts of NRI substrate are required for the attenuation of the load on the output protein NRI*, we performed time course experiments to assess the speed of response to aTc induction when the NRI substrate was increased. Fig. 4AB show the temporal response of GFP following induction with 16 nM aTc for the system with low NRI (L) and medium NRI (M) without load (Fig. 4A) and with load (Fig. 4B). The temporal response was substantially slower with increased amounts

of NRI substrate. Specifically, the system with medium NRI (M) without load suffered a 52% increase in response time as compared to the system with low NRI (L) without load. Similarly, the system with medium NRI (M) with load suffered a 27% increase in response time as compared to the system with low NRI (L) with load. (see Supplementary Fig. S10). Simulation results shown in the insets of Fig. 4 correlated well with experimental data. These observations confirm that the temporal response of an enzyme is slowed-down by its substrates in the cell just like it was reported *in vitro*.[26]

Hence, while increased amounts of NRI substrate are required for attenuating the steady state effects of DNA load on the output of the cycle, they lead to a slowdown of the overall system's temporal dynamics. This demonstrates a tradeoff between performance (speed of response) and robustness (to environmental load), which needs to be accounted for when designing these systems.

Interestingly, with high NRI (H), the system dynamics became marginally faster (Fig. S10). To investigate this phenomenon, we studied a simplified model in Supplementary Information, section 3.5.2. The model reveals that the total amount of NRI has two opposite effects on the kinase dynamics. On the one hand, increased amounts of total NRI tend to slow down the kinase dynamics as NRI acts as a load to the kinase. On the other hand, the total amount of NRI provides an effective feedback term in the kinase dynamics, that, becoming dominant at larger NRI concentrations, leads to a marginal speed up in the kinase dynamics. Since the dynamics of the GFP expression are dominated by the amount of NRI/DNA complex phosphorylation by NRII (see Supplementary Information, section 3.5.2), it is the speedup in the NRII dynamics that leads to the marginally faster dynamics of the GFP concentration.

While the DNA load substantially affects the steady state response of the system for very low and low values of NRI substrate, it did not show any major slow-down of the temporal dynamics of the system (Supplementary figures S5C,D and S10E,F). This is expected when the decay rate of the output TF (NRI*) is sufficiently large compared to the rate of change of the kinase.[5] The decay rate of NRI* results from dilution, phosphatase-mediated dephosphorylation, and spontaneous dephosphorylation. Since NRI* has a substantial autophosphatase activity, it has a large spontaneous dephosphorylation rate that results in a very short half-life of about 4 minutes.[23] This half-life is much smaller than the characteristic time scales of gene expression that control the temporal rate at which the kinase concentration increases. Hence, no load-induced slowdown was expected on the NRI* concentration.

5. Band-pass filtering of stimulus amplitude

There are various regulators that bind to their respective target DNA sites even before phosphorylation, though in many cases their affinity for target DNA increases after phosphorylation.[18, 27-29] It is well known that the NRI substrate can bind to the

GFP *glnA* promoter even in its unphosphorylated form with binding affinity similar to that of NRI*.[30] The cooperativity between neighboring NRI dimers is required for transcriptional activation and it increases by about a factor of 20 after its phosphorylation.[22] Based on these evidences, we constructed a simple analytical model in which the *glnA* promoter can be bound by both forms of NRI, but when NRI is bound, the promoter ultimately allows transcription at a low basal rate while when NRI* is bound, transcription occurs at a much higher rate (see Supplementary Information, section 2.2). This model reveals that in the presence of a fixed amount of NRII kinase, as the NRI substrate is increased, the *glnA2* promoter becomes predominantly bound by the unphosphorylated NRI. If the basal GFP activation brought about by the unphosphorylated NRI is larger than that due to the kinase-phosphorylated NRI, GFP expression increases monotonically with NRI's concentration. Conversely, if the basal transcription of GFP is smaller than that due to the kinase-phosphorylated NRI, GFP expression decreases as NRI's concentration increases. That is, for low values of NRI the GFP expression increases with NRI until a maximal expression is reached after which, further increase of NRI leads to a reduction of GFP expression. That is, the response of GFP concentration to the total amount of NRI substrate is biphasic when the concentration of kinase is sufficiently high. When the concentration of kinase is low, the activation of GFP is predominantly due to increasing values of NRI unphosphorylated, which monotonically increases with the total amount of NRI substrate. In this case, the response of GFP to the total amount of NRI substrate is monotonic.

Figure 5 shows experimental and simulation data of fluorescence as a function of the amounts of NRI substrate. As expected, for low amount of kinase (2 nM aTc), there was a monotonically increasing relationship between NRI substrate concentration and GFP (Fig 5A). By contrast, at higher amounts of kinase, the system behaved in a biphasic manner with increasing concentrations of NRI substrate (Fig. 5B,C and Supplementary Fig. S11). Simulation data correlates well with experiments and is obtained from a detailed ODE model of the system (Supplementary Information, section 3.3). The biphasic behavior is preserved in systems with DNA load, indicating that it is a robust characteristic to interactions with environment's binding sites. Such biphasic behaviors have been explained before for various motifs in regulatory networks such as feedforward loops or ligands acting both as activators and repressors of a receptor depending on their oligomerization state.[31, 32] In our system, the phenomenon is due to the kinase saturation by the substrate combined with the binding of unphosphorylated substrate to the promoter. The former limits the amounts of phosphorylated protein achievable for any kinase concentration, while the latter leads to sequestration of the promoter from the phosphorylated protein. Therefore, phosphorylation motifs where the unphosphorylated substrate can bind to the DNA promoter without significant activation can function as band-pass filters that select input stimuli only around a desired amplitude level.

In this paper, we have designed and fabricated an amplifying buffer circuit in *E. coli,* which enables to achieve desired input/output signal amplification while

attenuating the effect of DNA load on the output. This type of design allows to insulate the input/output response of a genetic device from the potentially large number of (unknown) interactions between the output TF and binding sites in the cellular environment, thus making the device function essentially independent of the cellular context.

We have shown that the ability of insulating the system from retroactivity to the output due to DNA load comes with an expense of a slower input/output dynamic response, a tradeoff that needs to be taken into account in the design. This type of tradeoff appears to be a fundamental limitation of single phosphorylation cycles,[33] but can be overcome by having multiple stages of phosphorylation in a cascade.[34] In this case, the fast phosphorylation reaction of the stage before the last can compensate for the slow down due to the load applied by the large amount of substrate in the last stage. Hence, multiple stages of phosphorylation would allow insulating the input/output response from DNA load while keeping a fast input/output temporal dynamics.

While TCS motifs provide remarkable flexibility in tuning the input/output response in a genetic device, the design and fabrication of synthetic genetic circuits that incorporate TCS systems is still fairly limited. Previous work has demonstrated that it is possible to control the specificity of TCS systems and that they can provide a suitable platform for programming signal transduction in bacteria.[35, 36] Our work adds to these results demonstrating that TCS can be tuned with high flexibility and employed in genetic circuits to realize a fundamental building block: the amplifying buffer.

Interestingly, most natural TCSs have cognate SK and RR pair whose genes are often positioned and expressed in tandem from the genome, and NtrB/NtrC is a typical example.[13] Their co-expression possibly leads to a better balance of the enzyme/substrate (SK/RR) ratio in comparison to other enzymes and substrates that are not co-expressed. Our experiments have demonstrated that increased amounts of the RR lead to retroactivity on the SK, slowing down its temporal dynamics. Hence, a system in which the amounts of SK are proportionally increased with the amounts of RR should mitigate load-induced slow down, providing a possible explanation to why SK and RR pairs are often expressed in tandem. Natural RR are often responsible for activating many downstream genes[13] by binding to multiple promoter DNA sites after phosphorylation. Many such RR also possess autophosphatase activity,[37] which provides the required speedup in temporal response to mitigate load-induced slow-down due to binding to DNA sites. These facts suggest that prokaryotic cells may have already been using TCS systems as natural amplifying buffers, allowing RR to robustly regulate large numbers of downstream targets and guarantee some level of modularity, which may carry evolutionary advantages.[38]

When creating future systems composed of multiple modules, a designer will have to examine each interconnection through available modeling tools, as described by

Gyorgy and Del Vecchio,[39] in order to assess potential loading problems. When loading is a problem, an insulation device, such as the amplifying buffer proposed here, will be chosen from a library. This device should have processes orthogonal to those of already inserted insulation devices. The potential ability of creating multiple orthogonal insulation devices is given by the existence of hundreds of orthogonal TCSs,[40] and by the fact that these can be used at the same time with minimal crosstalk.[36] Similarly, many orthogonal promoter-regulator pairs have been *de novo* synthesized and could be used to provide the required tuning of the gains.[41] Scaling up the size of synthetic circuits will also require mitigating the effects of depletion of key resources such as transcriptional and translational machinery, enzymes, and ATP.[42] Promising results have been obtained in this direction through the use of orthogonal transcription and translation resources to mitigate the impact of synthetic circuits on cell fitness.[43, 44]

MATERIALS AND METHODS

Circuit construction
For constructing the complete circuits, each gene in the circuit was sub-cloned with the appropriate promoter and ribosome binding site (RBS) upstream of it and with a double terminator to its downstream. The sub-cloning of each gene was performed using the BioBrick strategy (http://parts.igem.org/Main_Page) and each of the composite genes was cloned in a BioBrick compatible vector with ampicillin resistance marker gene for selection. All circuit parts with the exception of the substrate protein (NRI) have an LVA degradation tag in order to have faster dynamic response with increase in decay rate of the kinase and phosphatase. Since NRI is constitutively produced at a fixed level in all the circuits, no degradation tag was required for it. For more details on the design and construction of the circuits see Supplementary Information Sections 1.1 and 1.2.

Bacterial strains, media and growth conditions
All the DNA constructs in this study (including the partial/intermediate DNA constructs and complete biomolecular circuit plasmids) were transformed in NEB 5-alpha competent *E. coli* (high efficiency) (New England BioLabs Inc., USA). The circuit plasmids were transformed in the *E. coli* 3.300LGRKAPB mutant strain (see Supplementary Information Section 1.3 for the details of the strains) without and with DNA load plasmid. These cells were used for all the assays conducted in this study.

 Plasmids were isolated from the transformed strains using QIAprep spin mini-prep kit (QIAGEN, USA) after growing individual colonies in Luria Bertani medium at 37°C overnight. The complete circuits transformed in *E. coli* 3.300LGRKAPB strain were assayed after growing them in W-salts minimal medium (K_2HPO_4, 10.5 g; KH_2PO_4, 4.5 g; $MgSO_4$, 0.1 g; $(NH_4)_2SO_4$, 2 g; casaminoacids, 2 g; glucose, 4 g; glutamine, 2 g; glycine, 2 g; thiamine, 0.1 g in 1000 mL water). An overnight pre-culture of the circuit containing strains was prepared by growing individual colonies in 2 mL W-salts medium with appropriate antibiotics at 30°C and at 200 rpm in an orbital shaker.

Steady state and dynamics experiments
For determining the steady states for the circuits with varying NRI concentrations and with varying kinase, the individual colonies (3 representative colonies for 3 replicates) were grown as pre-culture. The main culture used in performing the induction assays was prepared after diluting the pre-culture and allowing it to grow for 10-12 h at 30°C and at 150 rpm (see Supplementary Information, section 1.5 for more details). Then cells were mixed with appropriate concentrations of the kinase inducer (aTc) in a total volume of 200 microliters and were added to a 96-well plate and were grown at 30°C in a plate reader with high shaking.

Flowcytometry analyses

Reporter analysis was conducted by measuring fluorescence of the super-folder GFP protein using a flow-cytometer. See Supplementary Information Section 1.6 for details.

Modeling and simulation
The modeling and simulation of the ODEs for the system was conducted using MATLAB. The detailed ODE model that we have developed considered a two-step reaction model for the kinase and phosphatase enzymatic reactions. The NRI substrate and NRII phosphatase have fixed expressions of the protein by constitutive promoters, while the NRII kinase was induced via aTc. The load and reporter promoters are conserved in this study. The half-life of NRI* is very low (~4 min) [23] and hence, its autophosphatase reaction is also considered in the model. The unphosphorylated dimers of NRI also bind to the target DNAs,[22] which is true for other RRs too, and hence we have incorporated this essential binding reaction for a more realistic model structure. Although NRI binds to the target DNA (P*glnA2* enhancer) with the same affinity as NRI*, transcriptional activation is brought about only after it is phosphorylated to form NRI*. Phosphorylation increases the cooperativity between the adjacent NRI dimers that leads to oligomerization and in turn brings about transcriptional activation and initiation.[22] The kinase and phosphatase enzymatic reactions are modeled also for the free and DNA-bound forms of NRI and NRI*, respectively. The details of all the ordinary differential equations (ODEs) of the reactions for the model are given in the Supplementary information sections 3.1 - 3.3.

AUTHOR CONTRIBUTIONS
KSN and DDV designed experiments; KSN and JJ performed experiments; KSN, PMR and DDV made mathematical models and performed simulations; KSN, JJ, PMR and DDV analyzed the data and wrote the manuscript.

CONFLICTS OF INTEREST
The authors declare no conflicts of interest.

SUPPLEMENTARY INFORMATION
The ODE for the model and the plasmid DNA sequences are given in the Supplementary Information section. The supplementary information can be downloaded from http://www.

REFERENCES

1.   Purnick, P. E., and Weiss, R. (2009) The second wave of synthetic biology: from modules to systems, *Nature reviews. Molecular cell biology 10*, 410-422.
2.   Lou, C., Stanton, B., Chen, Y. J., Munsky, B., and Voigt, C. A. (2012) Ribozyme-based insulator parts buffer synthetic circuits from genetic context, *Nature biotechnology 30*, 1137-1142.
3.   Bashor, C. J., and Collins, J. J. (2012) Insulating gene circuits from context by RNA processing, *Nature biotechnology 30*, 1061-1062.
4.   Burger, A., Walczak, A. M., and Wolynes, P. G. (2010) Abduction and asylum in the lives of transcription factors, *Proc Natl Acad Sci U S A 107*, 4016-4021.
5.   Del Vecchio, D., Ninfa, A. J., and Sontag, E. D. (2008) Modular cell biology: retroactivity and insulation, *Molecular systems biology 4*, 161.
6.   Jayanthi, S., Nilgiriwala, K. S., and Del Vecchio, D. (2013) Retroactivity controls the temporal dynamics of gene transcription, *ACS Synth Biol 2*, 431-441.
7.   Lee, T. H., and Maheshri, N. (2012) A regulatory role for repeated decoy transcription factor binding sites in target gene expression, *Molecular systems biology 8*, 576.
8.   Buchler, N. E., and Louis, M. (2008) Molecular titration and ultrasensitivity in regulatory networks, *J Mol Biol 384*, 1106-1119.
9.   Brewster, R. C., Weinert, F. M., Garcia, H. G., Song, D., Rydenfelt, M., and Phillips, R. (2014) The transcription factor titration effect dictates level of gene expression, *Cell 156*, 1312-1323.
10.   Saez-Rodriguez, J., Kremling, A., and Gilles, E. D. (2005) Dissecting the Puzzle of Life: Modularization of Signal Transduction Networks, *Computers & Chemical Engineering 29*, 619-629.
11.   Cardinale, S., and Arkin, A. P. (2012) Contextualizing context for synthetic biology – identifying causes of failure of synthetic biological systems, *Biotechnology Journal 7*, 856-866.
12.   Schaller, G. E., Shiu, S. H., and Armitage, J. P. (2011) Two-component systems and their co-option for eukaryotic signal transduction, *Current biology : CB 21*, R320-330.
13.   Yamamoto, K., Hirao, K., Oshima, T., Aiba, H., Utsumi, R., and Ishihama, A. (2005) Functional characterization in vitro of all two-component signal transduction systems from Escherichia coli, *Journal of Biological Chemistry 280*, 1448-1456.
14.   Foussard, M., Cabantous, S., Pédelacq, J.-D., Guillet, V., Tranier, S., Mourey, L., Birck, C., and Samama, J.-P. (2001) The molecular puzzle of two-component signaling cascades, *Microbes and infection 3*, 417-424.
15.   Miller, S. I., Kukral, A. M., and Mekalanos, J. J. (1989) A two-component regulatory system (phoP phoQ) controls Salmonella typhimurium virulence, *Proceedings of the National Academy of Sciences 86*, 5054-5058.
16.   Nixon, B. T., Ronson, C. W., and Ausubel, F. M. (1986) Two-component regulatory systems responsive to environmental stimuli share strongly

conserved domains with the nitrogen assimilation regulatory genes ntrB and ntrC, *Proceedings of the National Academy of Sciences 83*, 7850-7854.

17. Bernardini, M., Fontaine, A., and Sansonetti, P. (1990) The two-component regulatory system ompR-envZ controls the virulence of Shigella flexneri, *Journal of bacteriology 172*, 6274-6281.

18. Leonhartsberger, S., Huber, A., Lottspeich, F., and Bock, A. (2001) The hydH/G Genes from Escherichia coli code for a zinc and lead responsive two-component regulatory system, *J Mol Biol 307*, 93-105.

19. Jiang, P., and Ninfa, A. J. (1999) Regulation of Autophosphorylation of Escherichia coli Nitrogen Regulator II by the PII Signal Transduction Protein, *Journal of bacteriology 181*, 1906-1911.

20. Zimmer, D. P., Soupene, E., Lee, H. L., Wendisch, V. F., Khodursky, A. B., Peter, B. J., Bender, R. A., and Kustu, S. (2000) Nitrogen regulatory protein C-controlled genes of Escherichia coli: scavenging as a defense against nitrogen limitation, *Proc Natl Acad Sci U S A 97*, 14674-14679.

21. Ninfa, A., Atkinson, M., Forger, D., Atkins, S., Arps, D., Selinsky, S., Court, D., Perry, N., and Mayo, A. (2009) A Synthetic Biology Approach to Understanding Biological Oscillations: Developing a Genetic Oscillator for Escherichia coli, In *Bacterial Circadian Programs* (Ditty, J., Mackey, S., and Johnson, C., Eds.), pp 301-329, Springer Berlin Heidelberg.

22. Weiss, V., Claverie-Martin, F., and Magasanik, B. (1992) Phosphorylation of nitrogen regulator I of Escherichia coli induces strong cooperative binding to DNA essential for activation of transcription, *Proc Natl Acad Sci U S A 89*, 5088-5092.

23. Weiss, V., and Magasanik, B. (1988) Phosphorylation of nitrogen regulator I (NRI) of Escherichia coli, *Proceedings of the National Academy of Sciences 85*, 8919-8923.

24. Pioszak, A. A., and Ninfa, A. J. (2003) Genetic and biochemical analysis of phosphatase activity of Escherichia coli NRII (NtrB) and its regulation by the PII signal transduction protein, *J Bacteriol 185*, 1299-1315.

25. Atkinson, M. R., and Ninfa, A. J. (1993) Mutational analysis of the bacterial signal-transducing protein kinase/phosphatase nitrogen regulator II (NRII or NtrB), *J Bacteriol 175*, 7016-7023.

26. Jiang, P., Ventura, A. C., Sontag, E. D., Merajver, S. D., Ninfa, A. J., and Del Vecchio, D. (2011) Load-induced modulation of signal transduction networks, *Science signaling 4*, ra67.

27. Ellison, D. W., and McCleary, W. R. (2000) The unphosphorylated receiver domain of PhoB silences the activity of its output domain, *J Bacteriol 182*, 6592-6597.

28. Gusa, A. A., and Scott, J. R. (2005) The CovR response regulator of group A streptococcus (GAS) acts directly to repress its own promoter, *Mol Microbiol 56*, 1195-1207.

29. Matta, M. K., Lioliou, E. E., Panagiotidis, C. H., Kyriakidis, D. A., and Panagiotidis, C. A. (2007) Interactions of the antizyme AtoC with regulatory elements of the Escherichia coli atoDAEB operon, *J Bacteriol 189*, 6324-6332.

30. Shiau, S. P., Schneider, B. L., Gu, W., and Reitzer, L. J. (1992) Role of nitrogen regulator I (NtrC), the transcriptional activator of glnA in enteric bacteria, in reducing expression of glnA during nitrogen-limited growth, *J Bacteriol 174*, 179-185.

31. Kim, D., Kwon, Y. K., and Cho, K. H. (2008) The biphasic behavior of incoherent feed-forward loops in biomolecular regulatory networks, *BioEssays : news and reviews in molecular, cellular and developmental biology 30*, 1204-1211.

32. Levchenko, A., Bruck, J., and Sternberg, P. (2004) Regulatory modules that generate biphasic signal response in biological systems, *Systems biology 1*, 139-148.

33. Rivera, P. M., and Del Vecchio, D. (2013) Optimal design of phosphorylation-based insulation devices, In *American Control Conference (ACC), 2013*, pp 3783-3789, IEEE.

34. Rivera, P. M., and Del Vecchio, D. (2014) Retroactivity Attenuation through Signal Transduction Cascades, In *American Control Conference (ACC), 2014 (to appear)*, IEEE.

35. Capra, E. J., and Laub, M. T. (2012) Evolution of two-component signal transduction systems, *Annu Rev Microbiol 66*, 325-347.

36. Whitaker, W. R., Davis, S. A., Arkin, A. P., and Dueber, J. E. (2012) Engineering robust control of two-component system phosphotransfer using modular scaffolds, *Proceedings of the National Academy of Sciences 109*, 18090-18095.

37. Gao, R., Mack, T. R., and Stock, A. M. (2007) Bacterial response regulators: versatile regulatory strategies from common domains, *Trends in biochemical sciences 32*, 225-234.

38. Kirschner, M. W., and Gerhart, J. C. (2006) *The plausibility of life: Resolving Darwin's dilemma*, Yale University Press.

39. Gyorgy, A., and Del Vecchio, D. (2014) Modular composition of gene transcription networks, *PLoS computational biology 10*, e1003486.

40. Laub, M. T., and Goulian, M. (2007) Specificity in two-component signal transduction pathways, *Annu. Rev. Genet. 41*, 121-145.

41. Rao, C. V. (2012) Expanding the synthetic biology toolbox: engineering orthogonal regulators of gene expression, *Current opinion in biotechnology 23*, 689-694.

42. An, W., and Chin, J. W. (2009) Synthesis of orthogonal transcription-translation networks, *Proceedings of the National Academy of Sciences 106*, 8477-8482.

43. Rackham, O., and Chin, J. W. (2005) A network of orthogonal ribosome·mRNA pairs, *Nature chemical biology 1*, 159-166.

44. Segall-Shapiro, T. H., Meyer, A. J., Ellington, A. D., Sontag, E. D., and Voigt, C. A. (2014) A 'resource allocator'for transcription based on a highly fragmented T7 RNA polymerase, *Molecular systems biology 10*.

FIGURE LEGENDS

Fig. 1 **Amplifying buffer concept**. (A) Schematic representation of the genetic layout of the amplifying buffer circuit. The output transcription factor X* results from the phosphorylation of a substrate X in total amount X_{tot} through the kinase Z, which is controlled by an inducible promoter by an input molecule U. The output transcription factor is dephosphorylated by a phosphatase Y in total amount Y_{tot}. The transcription factor can bind specifically or non-specifically to a large number of DNA binding sites (depicted in red), which, as a consequence, apply a load to the transcription factor. (B) Block diagram representation highlighting the physical entities responsible for the input amplification and the negative feedback of the amplifying buffer circuit. The total amount of substrate X_{tot} contributes to the amplification of the signal transmitted by Z while the negative feedback gain increases with the total amount of phosphatase Y_{tot}. The load appears as a disturbance that tends to decrease the output X*. Simple block diagram algebra leads to the expression of the concentration of X* on the right-hand, where we have assumed that Y_{tot} is sufficiently large such that $k_2 Y_{tot} >> 1$. As X_{tot} and Y_{tot} increase, the gain from Z to $X*$ can be kept to a desired value while decreasing the impact of the load on the same output $X*$.
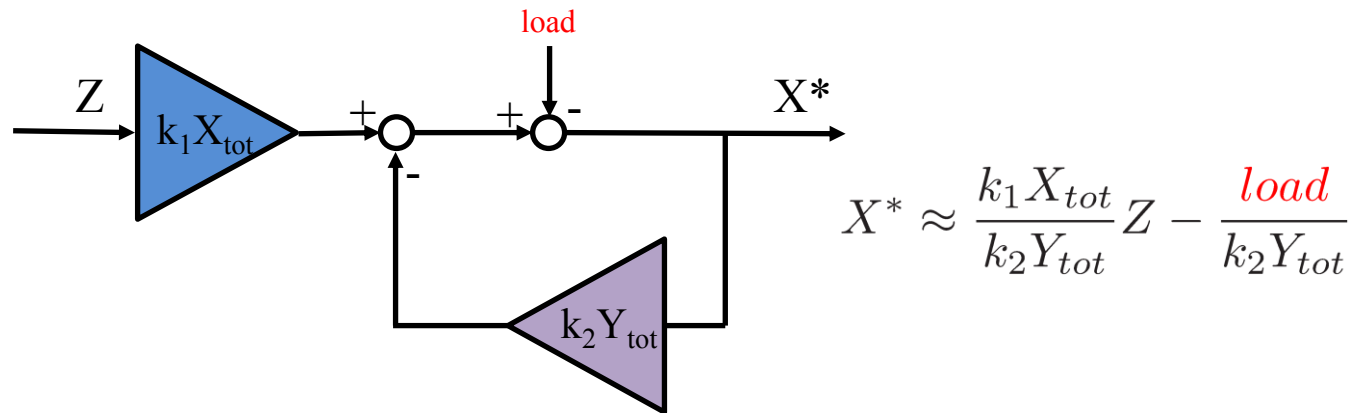
Fig. 2 **Amplifying buffer genetic circuit layout**. The amplifying buffer takes aTc (U) as an input and produces phosphorylated NRI (NRI*) as output X*. A constant amount of NRI substrate protein is constitutively expressed; whereas the kinase and phosphatase are regulated by TetR and LacI repressors, respectively, and are induced by aTc and IPTG, respectively. The phosphorylated NRI (NRI*) initiates transcription from the P*glnA2* promoter, which controls the expression of the reporter protein (superfolder GFP protein) from the sf-*gfp* gene cloned downstream of the promoter. All the circuit proteins have the degradation tag (LVA) except for the NRI substrate. The promoter P*const* upstream of *tetR* and *lacI* genes indicate a high strength constitutive promoter (BBa_J23114). The *Pconst** upstream of the gene *ntrC* represents variable constitutive promoters; for details refer to Supplementary Information, Table S5.

Fig. 3 **Dose response curves of the amplifying buffer circuit**. (A) For low amounts of NRI (L), the system with DNA load (red) showed a substantially lower steady state than the system without load (black) at all kinase concentrations. The error bars indicate standard deviation between the 3 replicates. (B) The circuit with medium amount of NRI (M) was considered. In this case, the presence of DNA load did not significantly affect the dose response curve, but the output is larger than in the original circuit in (A) for each input value of kinase. (C) Solid lines indicate the original system with low amounts of NRI (L) shown in (A), while dashed lines indicate the system with medium amounts of NRI (M) induced with 80 μm IPTG. The addition of IPTG lowers the steady state compared to the plots in (B) and brings the dose response curve to essentially overlap with that of the original circuit in (A),

which suffered due to the DNA load. Now, the system does not significantly suffer from the presence of DNA load since the black (no load) and red (with load) dose response curves overlap. Each point in the graphs is the mean fluorescence of the cells from three replicates and the error bars indicate standard deviation. (D) *Simulated data*. Simulation data obtained from the detailed ODE model (Supplementary Information, section 3.3).

Fig. 4 **Temporal dynamics**. The (10-90)% rise time of GFP expression after induction with a constant amount of aTc (16 nM aTc) was observed for different amounts of NRI substrate (low and medium). The normalized temporal responses are shown for the system without load in (A) and for the system with load in (B). The insets in the graphs show the simulation data obtained by the detailed ODE model (Supplementary Information, section 3.3). The response time increases for circuits with higher NRI independent of the DNA load.

Fig. 5 **Biphasic steady state response to NRI substrate**. The plots show steady state levels of GFP concentration for the circuits without (black)/with (red) DNA load and as a function of the concentration of NRI for varying kinase concentrations: (A) 2 nM aTc, (B) 4 nM aTc, and (C) 20 nM aTc. Each point in the graphs is the mean fluorescence of the cells from three replicates and the error bars indicate standard deviation. (C), (D), and (E) show simulation results obtained with the detailed ODE model explained in Supplementary Information, section 3.3. For additional aTc concentrations, refer to the Supplementary Information, section 1.4.

A

B

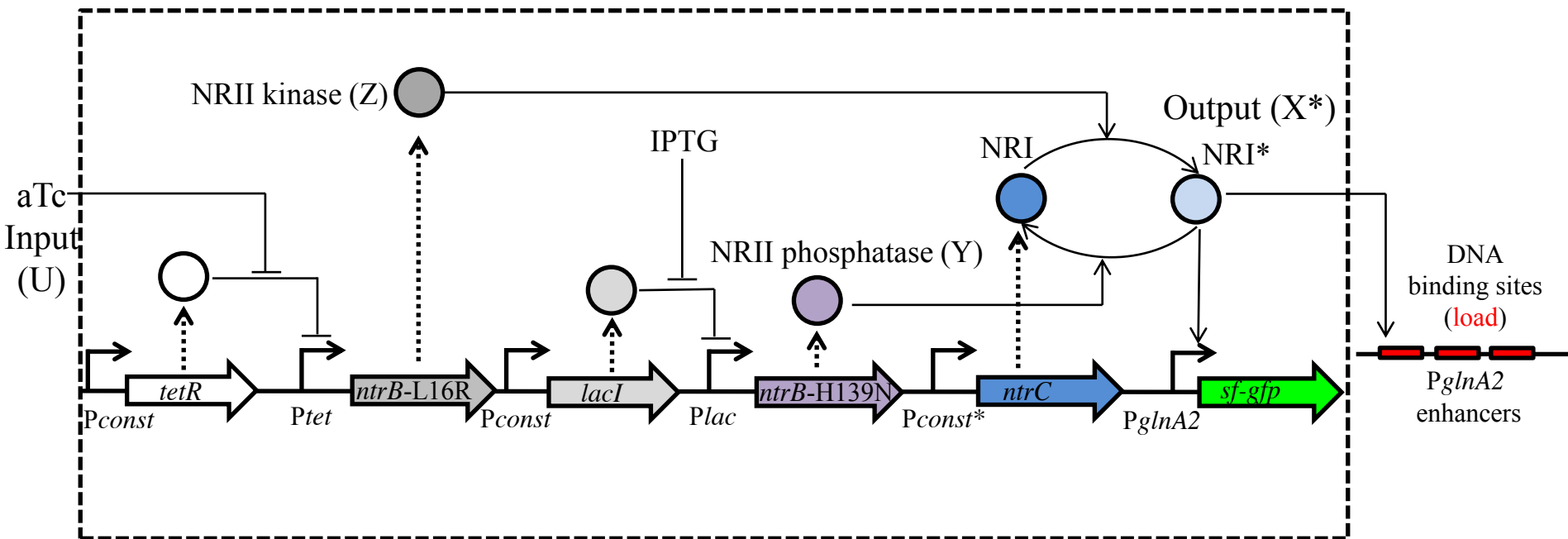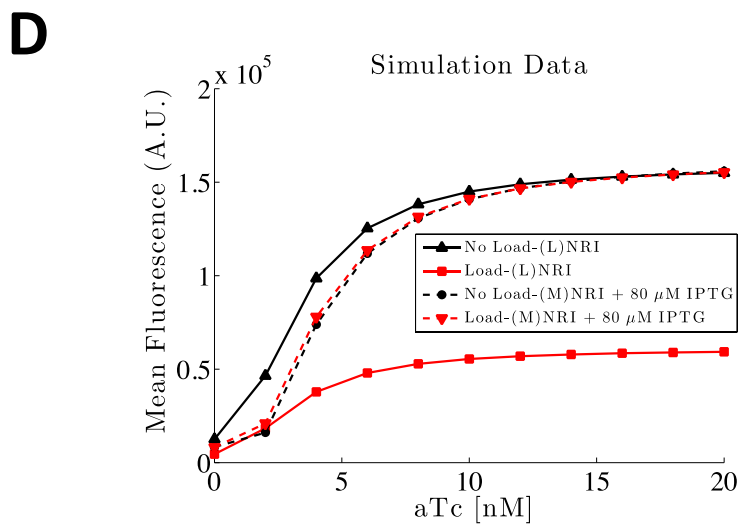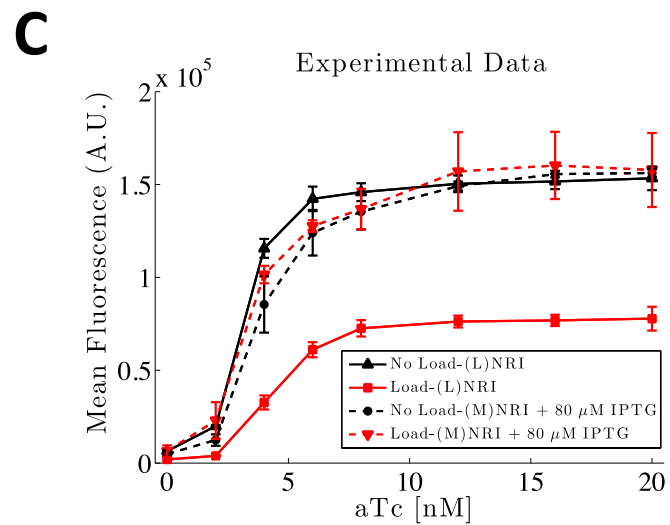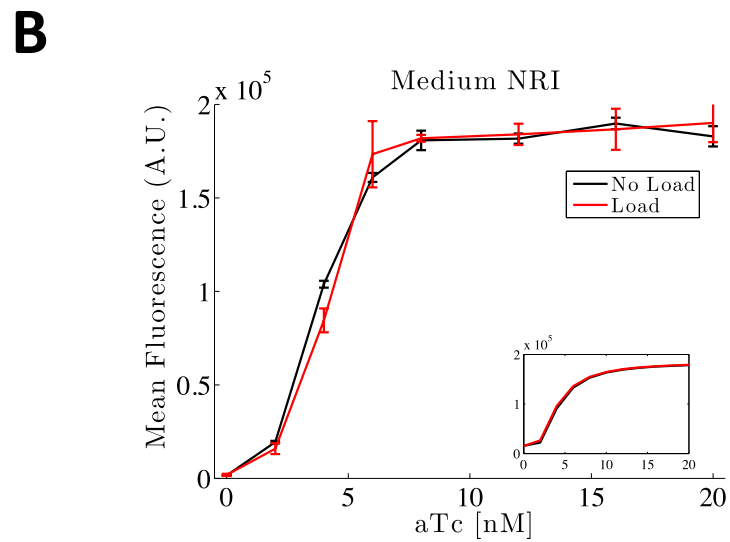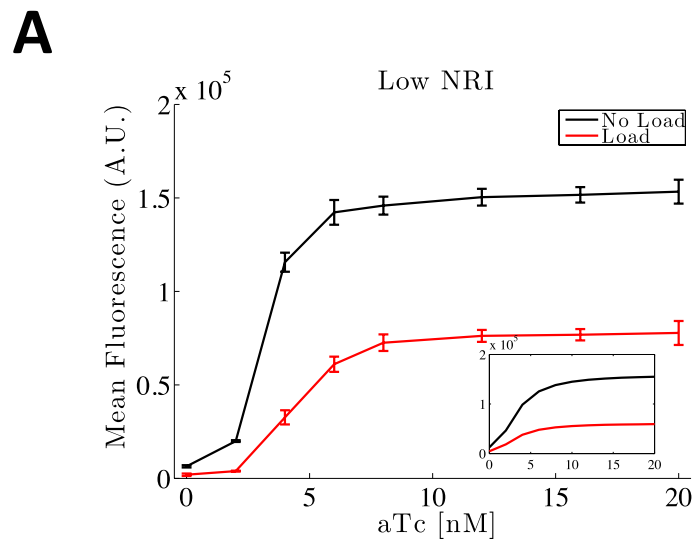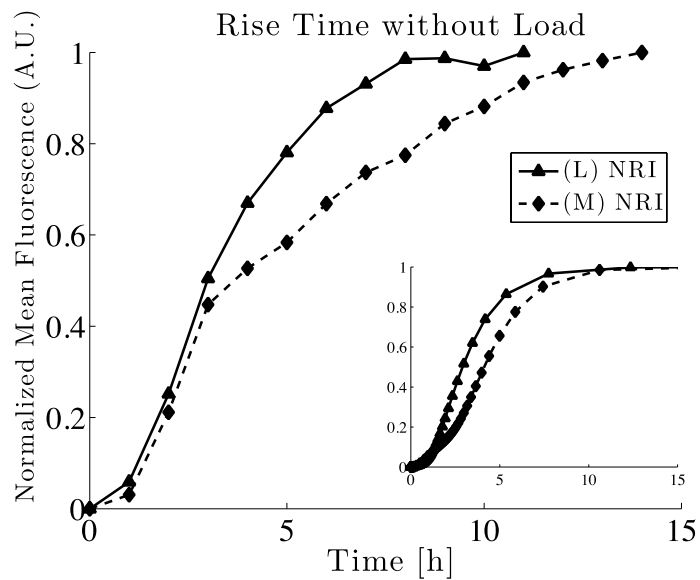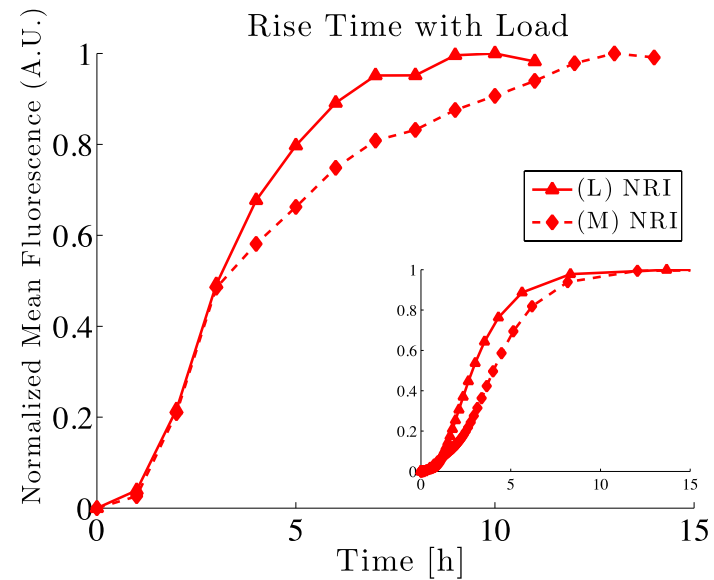$$X^* \approx \frac{k_1 X_{tot}}{k_2 Y_{tot}} Z - \frac{load}{k_2 Y_{tot}}$$

Figure 1

Figure 2

Figure 3

Figure 4

Figure 5